



Cite this: *J. Mater. Chem. C*,
2024, 12, 14551

Real-time and self-monitoring lubricant enabled by the triboluminescence of ZnS:Cu/GF/PTFE composites†

Xiuping Guo,^{ab} Wanyuan Wei,^a Xiao He,^c Fu Wang^a and Zhaofeng Wang   ^{abc}

Unexpected and fatal failure of vital dynamic components in machines happens every day, severely threatening human life and property. Therefore, the development of intelligent self-monitoring lubricants is highly required. In this work, we present a feasible approach to prepare a self-monitoring solid lubricating composite by introducing the triboluminescence (TL) material ZnS:Cu and the reinforced material glass fiber (GF) into a polytetrafluoroethylene (PTFE) solid lubricating material. The introduction of ZnS:Cu could achieve intense TL in the PTFE lubricating materials under mechanical stimuli with enhanced tribological properties. The produced TL signals during lubrication shows good responsiveness to the applied working parameters (load and velocity) with good stability and repeatability, confirming its desirable self-monitoring activities. The TL signal could also be employed to detect the service lifetime of the lubricating medium in solid–liquid lubrication systems. Furthermore, we constructed a TL bearing and simulated the operation process in space, which suggests that the as-fabricated ZnS:Cu/GF/PTFE lubricating composite shows particular application prospects in the aerospace field to ensure the stable and safe running of space equipment.

Received 5th June 2024,
Accepted 2nd August 2024

DOI: 10.1039/d4tc02309a

rsc.li/materials-c

1. Introduction

Friction and wear introduce significant uncertainties in machine reliability and performance, posing threats to human life and property. At present, nearly 23% of the world's total energy is consumed to overcome friction and remanufacturing worn-out parts.^{1–3} Lubricating materials could extend the lifetime of machines by reducing the friction between their components.^{4–6} Like the role of human blood in disease detection, the condition monitoring of lubricating materials offers crucial information for the early warning of machine failure.^{7,8} Lubricant condition monitoring can not only eliminate the need for costly machine shutdowns for inspection, but also minimize the risk of catastrophic component failure during operation. Therefore, it is highly required to develop effective monitoring and failure warning approaches for lubricating materials to ensure their safe operation and reduce the cost of maintenance.^{9,10}

Based on the physical state, lubricant monitoring is usually divided into lubricating oil condition monitoring and solid lubricant monitoring. Over the past decades, there have been remarkable advancements in lubricating oil monitoring. Since oxidation, wear particle pollution and water pollution are the main causes of the deterioration of lubricating oil, condition monitoring of these characteristics is effective to provide early warnings in failure progression. Ferrography and atomic emission spectroscopy could enable the identification of severe wear by detecting various wear particles in lubricating oil.^{11,12} Fourier transform infrared spectroscopy (FTIR), fluorescence spectroscopy and dielectric constant could determine the wear degree of oil by characterizing the viscosity, polarity and degradation of wear oil.^{13–15} Through the acoustic emission (AE) pulse count rate, the time-dependent behavior of grease lubrication in ball bearings could be monitored online under actual operating conditions.^{16,17} Recently, inspired by the working principle of triboelectric nanogenerators, lubricating oil could be self-powered to monitor the condition *in situ* through the shielding effect of abrasive dust and pollutants on electrical output characteristics.^{18,19} In addition to lubricating oil, solid lubricating materials have attracted much more attention during the past years because of their workable processability, chemical stability, corrosion-resistance, and wide temperature-range.^{20–23} To date, numerous studies from academia and industry have been conducted to monitor the state of

^a State Key Laboratory of Solid Lubrication, Lanzhou Institute of Chemical Physics, Chinese Academy of Sciences, Lanzhou, Gansu 730000, China.

E-mail: zhfwang@licp.ac.cn

^b Center of Materials Science and Optoelectronics Engineering, University of Chinese Academy of Sciences, Beijing 100049, China

^c Shandong Laboratory of Advanced Materials and Green Manufacturing at Yantai, Yantai, Shandong 265503, China

† Electronic supplementary information (ESI) available. See DOI: <https://doi.org/10.1039/d4tc02309a>



lubricating oil,^{18,24} but the development of an effective monitoring method for solid lubricating materials is still in the initial stages. Accelerated experiments could be used to predict the lifespan of solid lubricating materials and provide a probable time for part replacement.²⁵ However, it is difficult to deal with the sudden incidents during the practical operation. Real-time condition monitoring could be realized by collecting the friction coefficient signal of solid lubricating materials.²⁶ Surface plasmon resonance (SPR) with a gold-coated quartz prism could monitor the transfer films' wear *in situ* during sliding.²⁷ Recently, Choi and Wang' group realized self-powered and online monitoring of speed, friction coefficient and faults based on a triboelectric nanogenerator.^{28,29} However, the majority of the detecting systems for solid lubricants are bulky, and their short service life and high energy consumption pose challenges to downsizing and weight reduction. In addition, the above methods also have limitations in terms of the relatively low accuracy and signal delay. For these reasons, a novel lubricating monitoring approach with real time, *in situ*, self-powered, overly sensitive, self-diagnosis and self-warning characteristics is highly desired for the development of a new generation of intelligent lubricating materials.

Triboluminescence (TL) is a phenomenon where materials can emit light under the friction and rubbing stimuli.^{30–35} The unique mechanics-photon conversion of TL could realize the visualization and dynamic imaging/sensing of the friction parameters, with the advantages of non-destructiveness, wireless, convenience, and accurate detection.^{36–40} In addition to the *in situ* sensing/monitoring activities during friction, inorganic TL materials can also act as the reinforcing fillers to improve the mechanical and tribological performance of the polymer matrices.⁴¹ Therefore, combining inorganic triboluminescent powders with polymer solid lubricating materials may improve the wear resistance and simultaneously provide the possibility for the realization of real-time and self-powered condition monitoring of lubricating materials.

Herein, in this work, we prepared a novel self-powered and self-monitoring composite by compositing the triboluminescent powder ZnS:Cu into the typical self-lubricating material glass fibers/polytetrafluoroethylene (GF/PTFE). The obtained composite simultaneously exhibits desirable lubrication and TL performance. By studying the TL responsiveness of the solid lubricating composite toward the working parameters (*e.g.*, load and speed), the real-time and self-powered monitoring of the running state could be realized, which shows good stability and repeatability. Such activity could also be extended to monitor the service lifetime of the lubricating medium on the surface of the solid lubricating composite. Furthermore, the TL bearing is constructed, and the simulated operation processes suggest its application prospect in aerospace. This work not only provides an intelligent lubricating material with real-time and self-powered condition monitoring activity but also brings a novel idea to deal with the friction/mechanics-related issues in engineering, which shows valuable guidance in various fields to guarantee the safe operation of equipment and reduce the corresponding safety accidents and economic losses.

2. Experimental section

2.1. Materials

ZnS:Cu (D512CT) powders and glass fibers (GF) were purchased from Shanghai Keyan Photoelectric Technology Co., Ltd and Nanjing Glass Fiber Research Institute, respectively. Polyflon PTFE M-18F, with a size of 25 μm , was obtained from Daikin Industries Co., Ltd. Engine oil (SN 5W-30) was purchased from Sinopec Lubricants Co., Ltd. Trimethylolpropane (TMP 108A) was supplied by Beijing Xirunte Trading Co., Ltd, which was oxidized for different times at 200 °C. Anhydrous ethanol (EA) was provided by Tianjin Rionlon Bohua Pharmaceutical & Chemical Co., Ltd.

2.2. Synthesis of the ZnS:Cu/GF/PTFE composite

An optimized mass ratio (6.3 : 0.7 : 3) of PTFE, GF and ZnS:Cu particles were weighed into a beaker (250 mL), and then alcohol (150 mL) was poured into the beaker. The mixture was mechanically stirred at 1800 rpm to obtain a uniformly dispersed suspension. The suspension was pumped and filtered to obtain the ZnS:Cu/GF/PTFE mixture, which was dried at 60 °C for 24 h in an oven. After that, the mixture was frozen at 0 °C for 24 h and cold pressed at 50 MPa for 3 min. Then, the mixture was heated to 330 °C with a rate of 1 °C min⁻¹ in a muffle furnace, holding for 60 min. It was further heated to 375 °C at 0.75 °C min⁻¹ and kept for 130 min. After cooling to room temperature, the ZnS:Cu/GF/PTFE composite was obtained. The ZnS:Cu/GF/PTFE composite surface was sanded with 800 mesh and 1500 mesh sandpapers for 2 min, and then the sample was ultrasonically cleaned in a beaker filled with acetone for 1 min. The acetone on the surface of ZnS:Cu/GF/PTFE was dried at room temperature, and the sample was collected for the follow-up testing.

2.3. Tribological testing

ZnS:Cu/GF/PTFE was placed on a CSM friction machine for the tribological test. A friction test (pin-on-disk geometry; radius of running: 5 mm; normal load: 10 N; rotary speed: 200 rpm) was performed between ZnS:Cu/GF/PTFE and 304 stainless-steel with 1 mm radius, and the acquisition frequency and test time were 10 Hz and 2 h, respectively. As for the monitoring of the lubricating medium, deionized water, ethanol, TMP 108A (different oxidized time), and the engine oil (new and wasted oil) were dropped on the ZnS:Cu/GF/PTFE surface for friction testing and signal monitoring.

2.4. Characterization

The crystal structure of ZnS:Cu powders was characterized by an X-ray diffractometer (Smart APEXII) using Cu K α radiation ($\lambda = 1.54 \text{ \AA}$) with a step size of 0.02°, ranging from 10° to 80°. The morphology of ZnS:Cu particles and the surface and grinding crack of ZnS:Cu/GF/PTFE were observed by scanning electron microscopy (SEM) (JSM-6701F). The elemental composition of ZnS:Cu/GF/PTFE wear marks was characterized by energy dispersive spectrometry (EDS). Triboluminescence was collected by an optical fiber equipped onto a fluorescence



spectrophotometer (Omni300i, Zolix Instruments Co., Ltd), and the signal was *in situ* generated from a CSM (Tribometer 3, Switzerland) friction testing machine. Five regions of the sample wear mark were randomly selected, and the cross-sectional area (A) was measured using an optical interferometer (KOL-Tencer, MicroXAM-800). The wear rate (W) of the material can be calculated by the formula $W = V/SF = AL/SF$ (V , total wear volume; S , sliding distance; F , load; A , cross-sectional area of wear surface; L , sliding perimeter). The triboelectric potential was measured 15 mm above the sample surface using an electrostatic measuring probe (SK050, KEYENCE (Japan) Co., Ltd). The oxidized TMP 108A samples before and after rubbing were characterized by Fourier-transform infrared spectroscopy

(FTIR, Nexus 870, Nicolet). The digital photos were taken at room temperature by a Canon EOS-T3i camera.

3. Results and discussion

The structure of the self-monitoring solid lubricant is illustrated in Fig. 1a, which was fabricated from the triboluminescent powder ZnS:Cu, glass fibers and self-lubricating material PTFE through the processes of extraction filtration, cold pressing, and hot firing (Fig. S1, ESI†). The employed ZnS:Cu has a face-centered cubic structure involving the sphalerite ($F43m$) and wurtzite ($P63mc$) phases, as revealed in Fig. S2 (ESI†) and Fig. 1b. The morphology

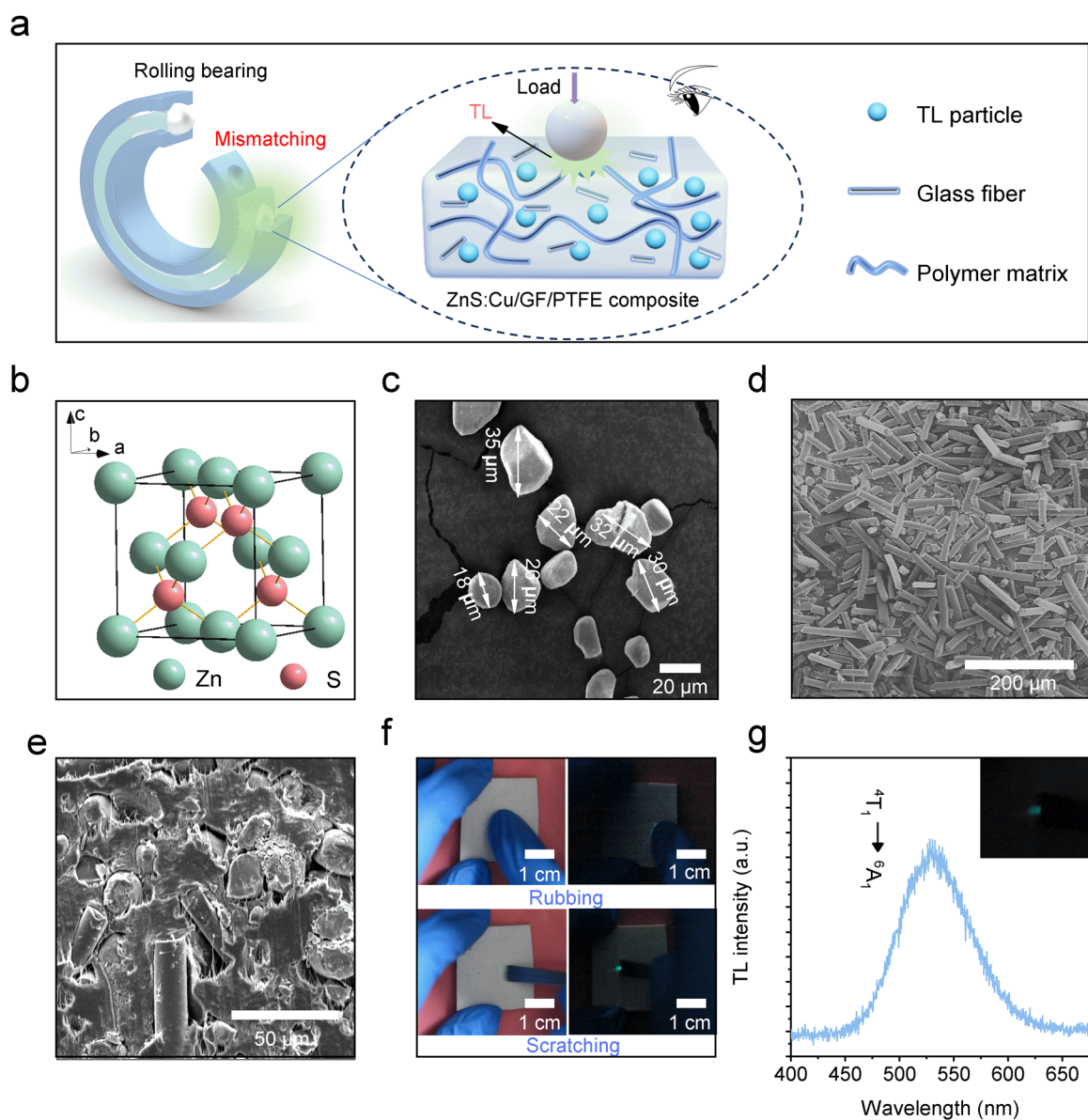


Fig. 1 Characterization of components of self-monitoring solid lubricant. (a) Schematic of the structure of the ZnS:Cu/GF/PTFE composite and its friction monitoring based on TL. (b) The crystal structure of ZnS. (c) SEM image of ZnS:Cu particles. (d) SEM image of glass fiber. (e) SEM image of the cross-sectional area of the ZGPC. (f) TL photographs of the ZGPC under friction stimulation. (g) TL spectrum of the ZGPC.



of ZnS:Cu is irregular with a size range from 20 to 40 μm , as shown in Fig. 1c. The employed glass fibers exhibit a rod morphology with an aspect ratio of 5:1–10:1, and the average diameter is *ca.* 20 μm (Fig. 1d). Fig. 1e shows the cross-sectional SEM image of the as-fabricated ZnS:Cu/GF/PTFE composite (ZGPC), which suggests that the ZnS:Cu irregular particles and glass fiber rods are well-distributed. The EDS images in Fig. S3 (ESI[†]) further confirm the uniform distribution of ZnS:Cu and glass fibers in PTFE. When the surface of ZGPC is rubbed by a finger or scratched by a metal sheet, intense green TL could be clearly observed with the naked eyes, as presented in Fig. 1f. The corresponding TL spectrum of ZGPC in Fig. 1g exhibits a broad emission peak at 523 nm, attributing to the characteristic $^4\text{T}_1$ to $^6\text{A}_1$ radiative transfer of Cu ions.

To evaluate the prospects of ZGPC for the self-monitoring lubricant applications, we further investigated its

triboluminescence and tribological properties specifically. As shown in Fig. 2a, the surface of ZGPC was rubbed with a pin (304 stainless-steel, diameter: 2 mm) to test its triboluminescence and tribological properties. Fig. 2b shows the photographs of ZGPC with different ZnS:Cu doping contents. It could be obviously observed that with the increase in ZnS:Cu, the TL intensity increases simultaneously, which is consistent with the corresponding spectral signal (Fig. 2c) and change trend of the fitted curve (Fig. 2d). This is because the TL of ZnS:Cu in the composites is mainly derived from triboelectricity between ZnS:Cu and PTFE.⁴² The more ZnS:Cu powders suffer from triboelectricity during the friction process, the higher the TL intensity. However, the further increase in ZnS:Cu doping contents would lead to a decrease in the plastic deformation (Fig. S4, ESI[†]) with the increased preparation cost.^{43–45}

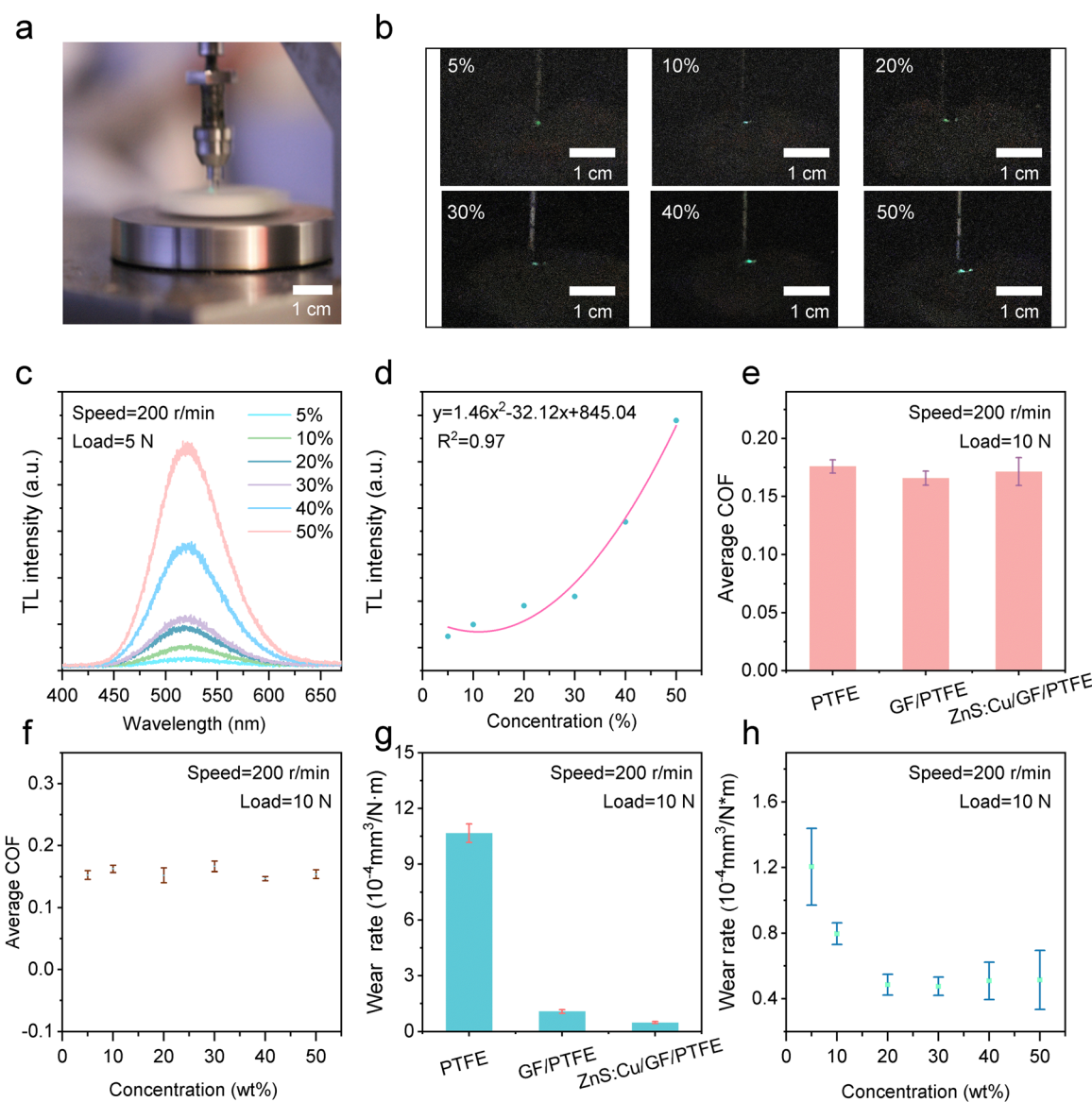


Fig. 2 The triboluminescence and tribological properties of the ZGPC. (a) Optical photograph of the *in situ* generation of TL signal on the ZGPC surface. (b)–(d) TL photographs, TL spectra, and corresponding relationship of ZGPC doping with different contents of ZnS:Cu. (e)–(h) The average coefficient of friction and wear rate of the PTFE-based composite at 200 rpm and 10 N.

In addition to the TL property, the influence of ZnS:Cu content on the tribological properties of solid lubricating material was also investigated. As shown in Fig. 2e, the addition of GF and ZnS:Cu has little influence on the friction coefficient of the PTFE composites. With the increase in the ZnS:Cu doping content, the friction coefficient shows no change (Fig. 2f). However, the wear rate of the PTFE composites could be significantly reduced with the doping of GF, while ZnS:Cu doping could further lower the wear rate. In Fig. 2g, as the contents of ZnS:Cu increase, the wear rate decreases significantly at the initial stage and then gradually stabilizes when the doping content reaches 30%. The concentration of GF

introduced into ZnS:Cu/PTFE has also been explored, and 7% is suggested to be the optimal doping concentration, as shown in Fig. S5 (ESI[†]). In comparison to pure PTFE, the wear rate of ZGPC is nearly one order of magnitude lower when the contents of GF and ZnS:Cu are 7% and 30%, respectively. Zn and Si elements are observed from the SEM and EDS images of grinding crack after rubbing for 2 h (Fig. S6, ESI[†]), indicating that ZnS:Cu and GF could preferentially support the load during friction to reduce the wear of PTFE.⁴⁶ Compared with traditional fillers, the doping of ZnS:Cu not only endows the solid lubricating materials with TL properties but also improves their wear resistance. Therefore, the resultant ZGPC holds

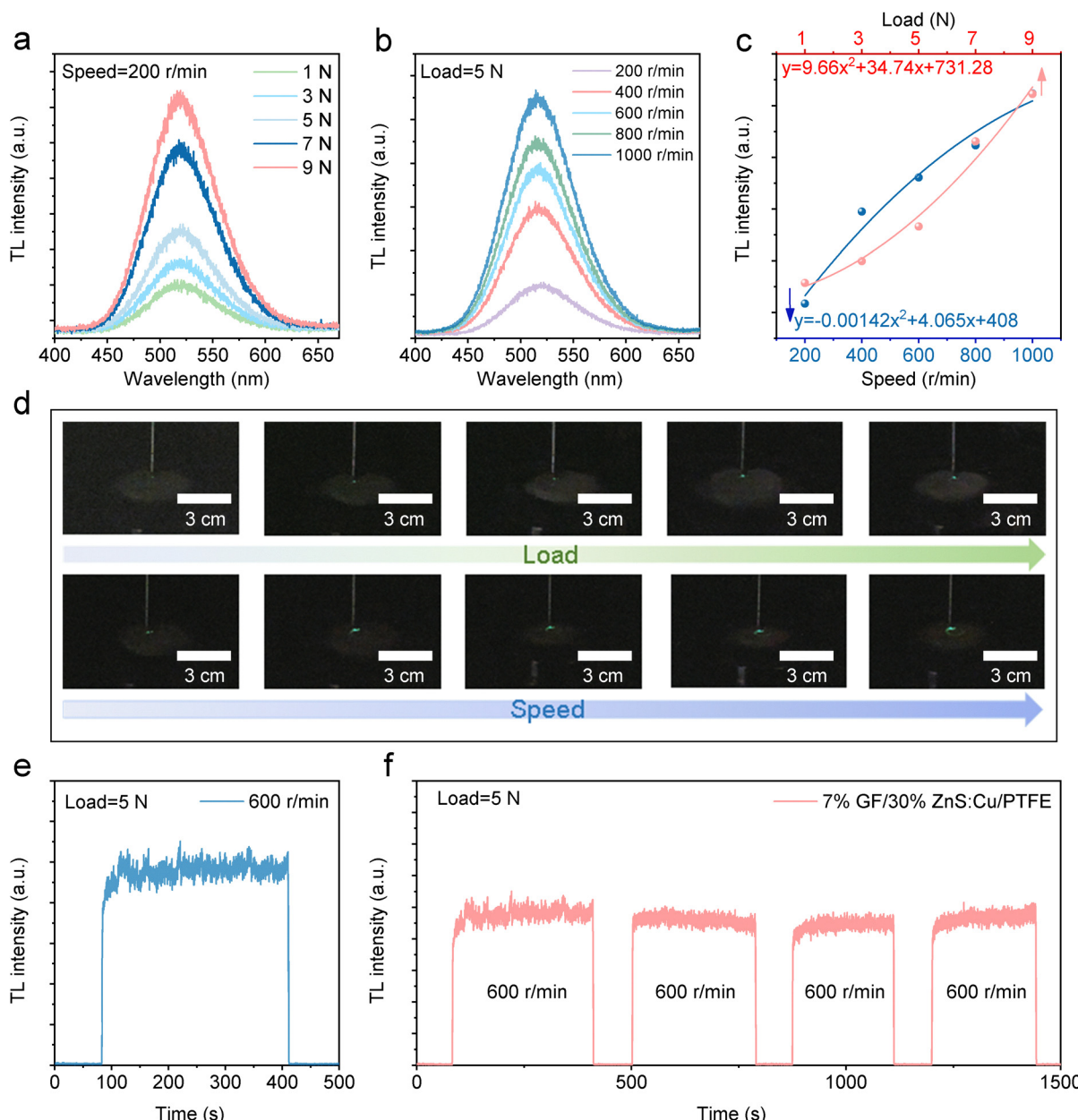


Fig. 3 The self-monitoring of ZGPC for load and rotational speed. (a) and (b) TL spectra of ZGPC under different loads and speeds. (c) and (d) The relationship and photographs between the TL intensity and the applied load or rotational speed. (e) Real-time monitoring of TL signals under 5 N and 600 rpm. (f) Repeatability test for TL monitoring.



immense potential in the realization of simultaneous self-monitoring and anti-attrition of the solid lubricating material.

Load and velocity are the most important parameters to reflect the abnormal contact during the friction process.⁴⁷ Fig. 3a and b present the TL spectra of ZGPC at different loads and rotational speeds. With the increase in the applied load from 1 N to 9 N, the TL intensity increases simultaneously (Fig. 3a). When the rotational speed varies from 200 to 1000 rpm, the larger rotational speed leads to higher TL intensity (Fig. 3b). The above TL intensity variation exhibits quadratic correlation to the applied friction load and rotational speed, as shown in Fig. 3c. The corresponding TL photographs

are presented in Fig. 3d. It should be noted that under the employed friction conditions for the above investigation, the average friction coefficient between stainless steel and ZGPC is stabilized at 0.15–0.175, suggesting its normal lubricating condition (Fig. S7a and b, ESI[†]). Therefore, the observed correlation between the TL signal and the applied load or rotational speed are valuable and appropriate for the self-powered condition monitoring when the sample is in a normal lubricating state. To understand the lubricating condition-induced TL intensity variation, the surface triboelectric potential between stainless steel and ZGPC was further investigated. As shown in Fig. S8 (ESI[†]), the absolute value of surface triboelectric

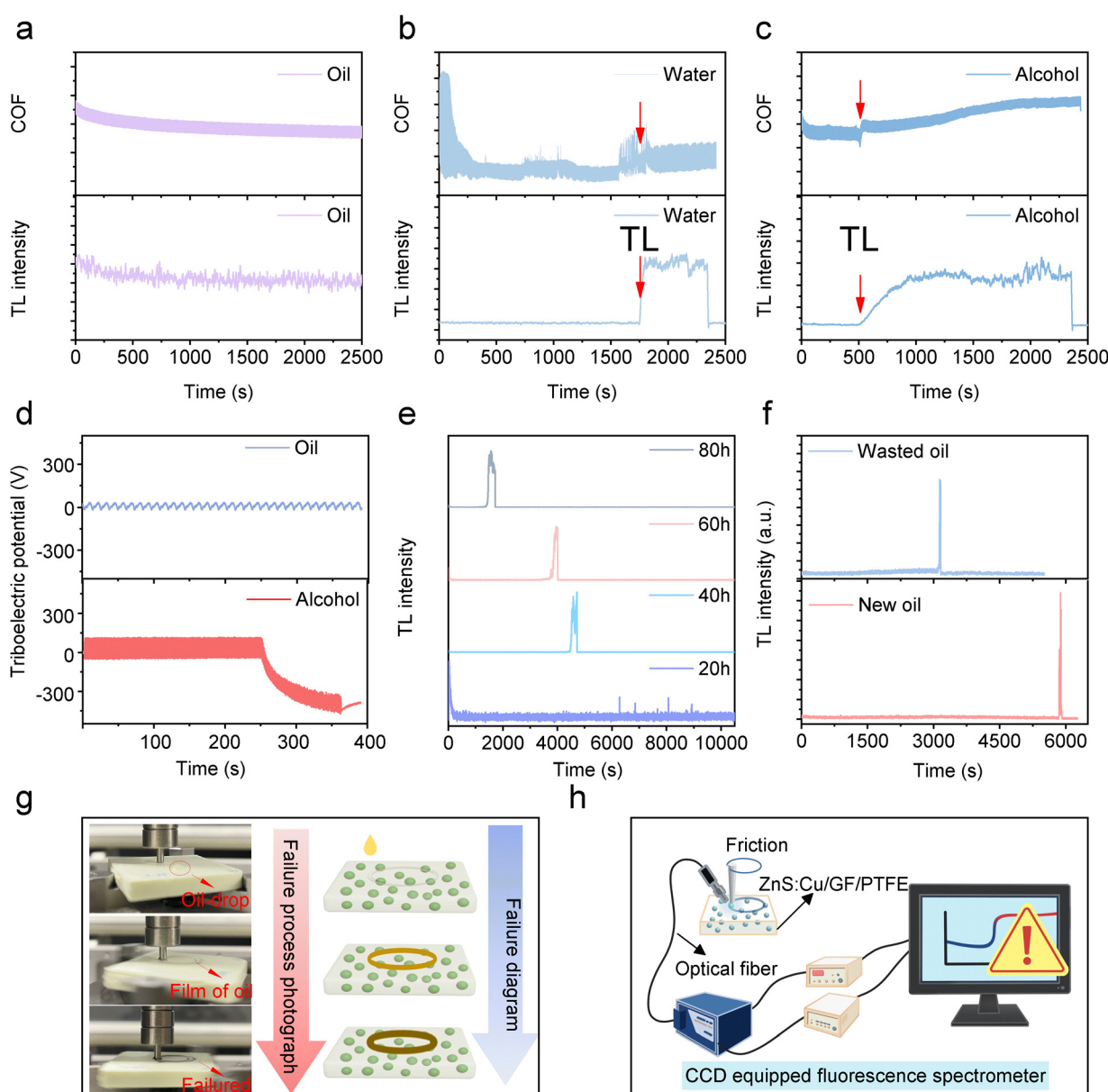


Fig. 4 Real-time self-monitoring of the ZGPC in solid–liquid composite lubrication. (a)–(c) The TL intensity and corresponding COF of the ZGPC surface with different lubricating mediums. (d) The triboelectric potential on the ZGPC with different surface mediums. (e) Real-time monitoring of TL signals of TMP 108A with different oxidation times under 15 N and 1000 rpm. (f) Real-time monitoring of TL signals of engine oil (SN 5W-30) and waste engine oil under 15 N and 1000 rpm. (g) Digital photographs of engine oil in service. (h) A schematic of the lubricating oil life monitoring system.



potential gradually increases with the increase in the applied load and rotational speed. Because the TL of ZnS:Cu in the composites is mainly derived from triboelectricity under mechanics, the increased surface triboelectric potential would then improve the TL intensity. In addition, higher rotational speed could also allow more photons to be detected to enhance the TL intensity because spectral capturing is actually operated under a certain integral time.

Stability and repeatability are two crucial parameters to evaluate the effectiveness and reliability of the sensors. Stability refers to the fluctuation degree of the measurement result within a certain time range. Repeatability or reproducibility means that the sensor can be used multiple times. The higher the stability and repeatability of the sensor, the higher the accuracy and reliability of the measurement results. Therefore, it is essential to investigate the stability and repeatability for evaluating the self-monitoring performance of ZGPC. As shown in Fig. 3e, under an optimal monitoring wavelength of 523 nm, the TL intensity of the composite exhibits a stable output signal for over 300 s at an applied load of 5 N and a high rotational speed of 600 rpm. The slight fluctuation of TL signals under friction demonstrates the stability of self-monitoring. Furthermore, the TL intensity remains steady even after many repeated on/off cycles (5 N, 600 rpm) in Fig. 3f, which indicates that ZGPC exhibits relatively accurate and repeatable self-monitoring performance. The above results suggest that ZGPC shows practicable and reliable self-monitoring activity with desirable stability and repeatability.

In addition to the load and velocity self-monitoring, the TL of ZGPC could also be employed to sense the lubricating medium on the solid lubricating material. As shown in Fig. 4a-c, the equal-volume lubricating oil, deionized water, and alcohol were separately dropped on the surface of ZGPC, which were then rubbed on the CSM friction machine. It is found that the lubricating oil dropped surface shows a stable friction coefficient of 0.0765 and no TL after rubbing for 2500 s. However, the TL signal appears on the ZGPC surface covered by deionized water and ethanol, with the friction coefficient of the surface changing abruptly from 0.0671 to 0.0915 and from 0.1252 to 0.1419, respectively. This should be caused by the different service life of the lubricating medium. Water and alcohol show a shorter service life due to their low boiling point, which would cause gradual evaporation during rubbing with a loss of carrying capacity or lubrication. Thus, the direct contact and friction between stainless steel and ZGPC could generate TL when the carrying capacity or lubrication of water and alcohol is lost. To further verify this viewpoint, we measured the triboelectric potential of the lubricating oil-dropped surface and the alcohol-dropped surface with a triboelectric potential measurement probe fixed at a height of 15 cm under a load of 4 N and a rotational speed of 60 rpm. As shown in Fig. 4d, the triboelectric potential on the lubricating oil dropped surface is almost unvaried, while the absolute value of triboelectric potential dropped alcohol increases significantly. The results suggest that the loss-carrying capacity of the alcohol dropped surface could facilitate TL generation on

ZGPC. Furthermore, TMP 108A with different thermal oxidation times was also employed to investigate the correlation between the service life of lubricating oil and the TL signal. The FTIR spectra of the oxidized TMP 108A before and after rubbing are provided in Fig. S9 (ESI†). The significantly enhanced absorption at 3525 cm^{-1} after rubbing indicates the increased concentration of carboxyl groups, suggesting that the oxidized TMP 108A is further degenerated and loses the carrying capacity. As shown in Fig. 4e, the appearance time of the TL signal is shortened by extending the oxidization time of dropped TMP 108A, confirming its applicability for lubricant monitoring. Moreover, the service life of the commercial engine oil (SN 5W-30) with different degradation degrees was also monitored by the TL signal. Also, the high load (15 N) and speed (1000 rpm) were employed to accelerate the lubricating oil failure and shorten the test cycles. As shown in Fig. 4f, the TL signals of the new engine oil dropped surface were detected after 85 min of friction. But the TL signals of the surface dropped waste engine oil was detected after only 50 min, which was consistent with the variation trend of the TL signal of base oil with different degree of thermal oxidation. All of the above investigations demonstrate that the TL of the ZGPC is effective to monitor the service life of the lubricating mediums. Accordingly, a real-time lubricating medium life monitoring system is established, as shown in Fig. 4g and h. It is worth noting that the above system is basically suitable for solid-liquid composite lubrication monitoring. At present, the solid-liquid composite lubrication is well recognized as the most promising method for lubricating because of its enhanced lubricant efficiency by converting the traditional solid-solid contact into the solid-liquid contact.⁴⁸ Therefore, the TL-based intelligent monitoring method proposed in this work is in high demand with the development trend of lubrication by providing a guarantee for the reliability, stability and safety of the solid-liquid composite lubrication.

Solid lubricants have been widely used in aerospace and military fields, which require the vacuum system or other extreme environments. Therefore, it is necessary to explore the reliability and environmental adaptability of ZGPC for lubrication monitoring in these extreme conditions. Herein, we simulate the operation process of the bearings in space, and the light signals are used to guarantee the safe operation of the equipment (Fig. 5a). As shown in Fig. 5b, TL rolling bearing was constructed with a plastic (PVC) outer ring, a stainless-steel rolling body, and an inner ring made of ZGPC. The obvious green light could be captured by naked eyes in the ZGPC inner ring of the rolling bearing under an ultraviolet lamp (Fig. S10, ESI†), which indicates that the TL bearing with a luminescent inner ring has been obtained successfully. To verify the feasibility of self-monitoring of ZGPC in the bearings, we employed the ball-on-disk friction mode to simulate the bearing conditions. As shown in Fig. S11 (ESI†), the TL intensity of the ZGPC in this case also shows good responsiveness to the applied friction load and rotational speed. The data curves in Fig. 5c and d further suggest that the self-monitoring behavior of the ZGPC under the ball-on-disk mode is relatively consecutive and stable.



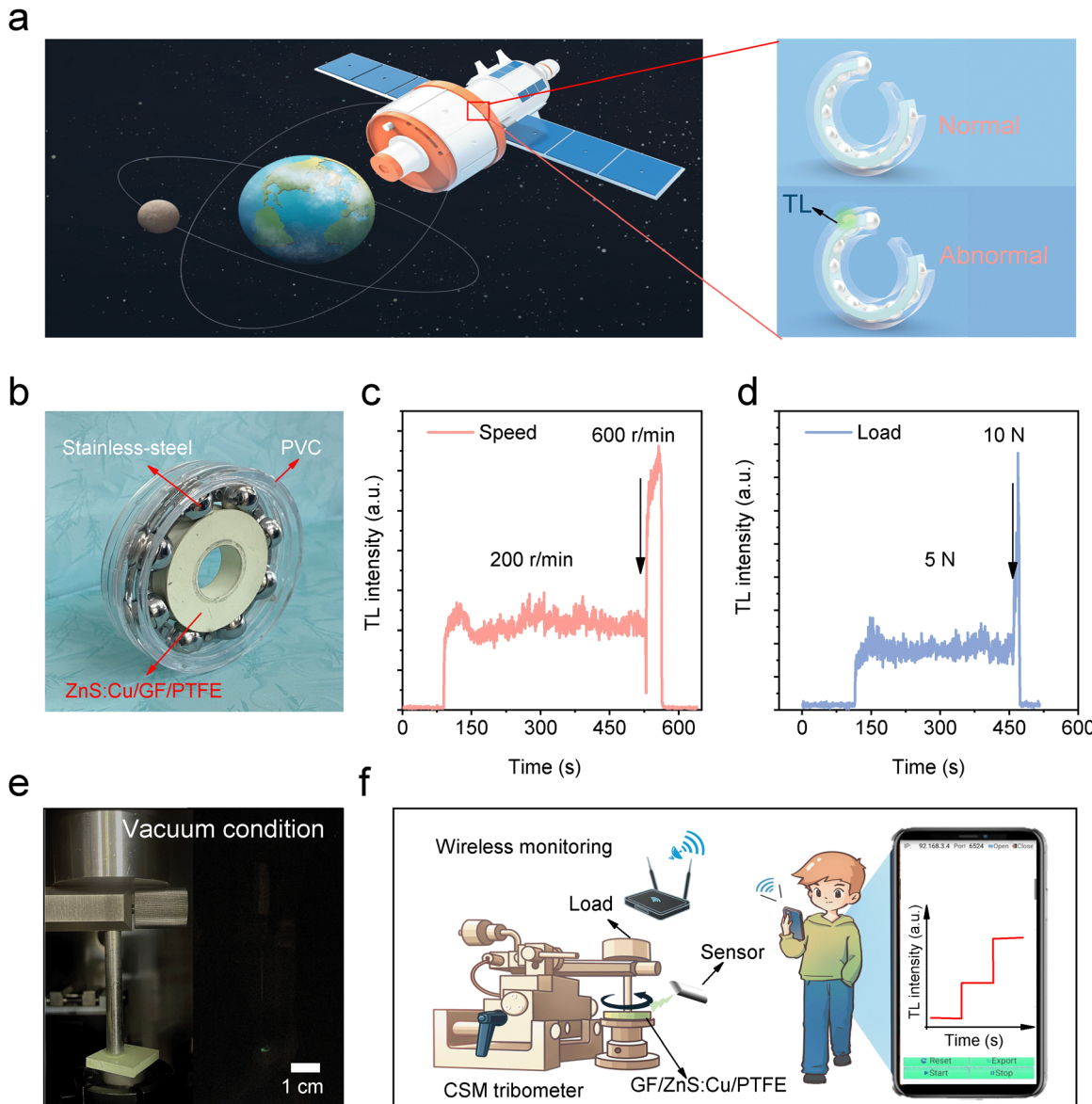


Fig. 5 Illustration of the self-monitoring of the ZGPC in aerospace. (a) Schematic of ZGPC application in the aerospace field. (b) Rolling bearing constructed using the ZGPC. (c) and (d) TL intensity monitoring of velocity and load under the ball-on-disk mode to simulate the bearing friction conditions. (e) TL photograph of the ZGPC under vacuum condition. (f) Schematic of the wireless transmission of TL signals from the ZGPC for real-time monitoring.

Moreover, when the ZGPC is placed under vacuum, it could still exhibit intense green TL with no obvious change compared to the one under atmospheric environment (Fig. 5e). These results suggest that the as-developed ZGPC are particularly appropriate for lubricant condition monitoring in aerospace bearings to ensure safe operation. Although the concept in terms of applying ZGPC in aerospace bearings is attractive, the practical applications should be more complicated due to the various working conditions and service environments.

Finally, we established a user-interactive system based on the lubricant self-monitoring performance of ZGPC. As illustrated in Fig. 5f, the easy-to-carry light intensity detector could capture the TL signal during operation and convert it to a

wireless Wi-Fi signal. Then, the Wi-Fi signal is accepted by a cellphone and converted to the lubricating information by the software. As a result, the lubricating conditions of the materials could be *in situ* and timely read out on the display screen. For a representative, the intelligent system for the self-monitoring of the rotational speed during lubrication under the ball-on-disk friction mode at the atmospheric environment is developed, as shown in Movie S1 (ESI†). The corresponding wireless signal could be received by the cellphone, and the rotational speed (200 rpm, 400 rpm and 600 rpm) of the lubricating system in the working state could be *in situ* and timely read out. These results further promote the applications of ZGPC with self-monitoring behavior.



4. Conclusions

In summary, we developed a self-monitoring ZGPC for the real-time intelligent diagnosis of solid lubricant by compositing ZnS:Cu and GF into a self-lubricating PTFE material. The doping of ZnS:Cu not only improves the wear resistance and maintains the friction coefficient of self-lubricating materials but also endows it TL property. It is found that the TL signals of ZGPC could sense the applied load and speed during the friction process. Meanwhile, by monitoring the TL signal, the service lifetime of the lubricating medium could also be monitored, which provides a pioneering approach to realize the self-monitoring of the running state of solid-liquid composite lubrication. Additionally, ZGPC was constructed into a bearing, and the simulated operations further suggests its self-monitoring ability in space. This work provides an intelligent self-monitoring solid lubricating material to diagnose the abnormal running state of machines, which brings a new idea to deal with the friction/mechanic-related issues in various fields. It should be noted that in the present work, the monitoring selectivity of the friction load and rotational speed has not been addressed yet. Future work by incorporating two kinds of TL powders with distinguished emission colour in the GF/PTFE lubricants may achieve the monitoring selectivity, and related work is under way.

Author contributions

Xiuping Guo: methodology, data curation, conceptualization, validation, investigation, formal analysis, and writing – original draft. Wanyuan Wei: validation, formal analysis, supervision, writing – review & editing, and funding acquisition. Xiao He: validation and investigation. Fu Wang: writing – review & editing, and funding acquisition. Zhaofeng Wang: conceptualization, supervision, validation, writing – review & editing, and funding acquisition.

Data availability

The data supporting this article have been included as part of the ESI.†

Conflicts of interest

There are no conflicts to declare.

Acknowledgements

This work was supported by the Strategic Priority Research Program of the Chinese Academy of Sciences (Grant No. XDB 0470201), the Technology Innovation Project for the Development of Instrument Testing and Analysis Methods of Lanzhou Regional Center, Chinese Academy of Sciences (Jz2024g102), the Natural Science Foundation of Gansu Province (23JRRA647), the Natural Science Foundation for Distinguished Young Scholars of Gansu Province (20JR5RA572), the Regional Development Young Scholar Program of the Chinese Academy of Sciences (E30283YRC1), and the Taishan Scholars Program.

Notes and references

- 1 H. P. Jost, *Lubrication (Tribology) - a report on the present position and industry's needs. Department of Education and Science*, H. M. Stationery Office, London UK, 1966.
- 2 K. Holmberg and A. Erdemir, *Friction*, 2017, **5**, 263.
- 3 L. Wang, D. Zhang, Z.-D. Luo, P. Sharma and J. Seidel, *Adv. Funct. Mater.*, 2023, **33**, 2303583.
- 4 B. C. Sharma and O. P. Gandhi, *Ind. Lubr. Tribol.*, 2008, **60**, 131.
- 5 Y. Han, D. Wu, J. Cheng, J. Wang, Y. Lu and X. Kong, *Prog. Nucl. Energy*, 2023, **166**, 104937.
- 6 B.-J. Jang, Q. Zhao, J.-H. Baek, J.-M. Seo, J.-P. Jeon, D. H. Kweon, G.-F. Han, C. Xu and J.-B. Baek, *Adv. Funct. Mater.*, 2023, **33**, 2306426.
- 7 C. Hu, W. A. Smith, R. B. Randall and Z. Peng, *Mech. Syst. Signal Proc.*, 2016, **76–77**, 319.
- 8 J. Zhu, J. M. Yoon, D. He, Y. Qu and E. Bechhoefer, *Int. J. Progn. Health Manage.*, 2013, **4**, 124.
- 9 R. Yan and R. X. Gao, *IEEE Trans. Instrum. Meas.*, 2004, **53**, 1327.
- 10 X. Zhu, C. Zhong and J. Zhe, *Tribol. Int.*, 2017, **109**, 473.
- 11 O. Levi and N. Eliaz, *Tribol. Lett.*, 2009, **36**, 17.
- 12 H. Wu, T. Wu, Y. Peng and Z. Peng, *Tribol. Lett.*, 2013, **53**, 411.
- 13 M. Wakiru, L. Pintelon, P. N. Muchiri and P. K. Chemweno, *Mech. Syst. Signal Proc.*, 2019, **118**, 108.
- 14 M. Sejkorová, B. Šarkan, P. Veselík and I. Hurtová, *Energies*, 2020, **13**, 6438.
- 15 P. Jia, F. Wang, W. Zeng and Z. Wang, *Anal. Methods*, 2022, **14**, 694.
- 16 J. Miettinen, P. Andersson and V. Wikström, *Proc. Inst. Mech. Eng., Part J*, 2001, **215**, 535.
- 17 I. A. Rastegaev, D. L. Merson, A. V. Danyuk, M. A. Afanasyev and A. Vinogradov, *Wear*, 2018, **410–411**, 83.
- 18 J. Zhao, D. Wang, F. Zhang, Y. Liu, B. Chen, Z. L. Wang, J. Pan, R. Larsson and Y. Shi, *ACS Nano*, 2021, **15**, 11869.
- 19 Y. Feng, X. Liu, Y. Lei, Z. Wu, L. Zhang, M. Feng, D. Wang and W. Liu, *Nano Energy*, 2024, **122**, 109304.
- 20 Y. Zhao, H. Mei, P. Chang, Y. Yang, L. Cheng and L. Zhang, *Composites, Part B*, 2021, **221**, 109013.
- 21 J. Zhang, D. Jiang, D. Wang, Q. Yu, Y. Bai, M. Cai, L. Weng, F. Zhou and W. Liu, *ACS Appl. Mater. Interfaces*, 2021, **13**, 58036.
- 22 H. Hu, Y. He, Q. Wang and L. Tao, *ACS Appl. Mater. Interfaces*, 2023, **5**, 6516.
- 23 K. E. V. Meter, C. P. Junk, K. L. Campbell, T. F. Babuska and B. A. Krick, *Macromolecules*, 2022, **55**, 3924.
- 24 L. Guan, X. L. Feng, G. Xiong and J. A. Xie, *Sens. Actuators, A*, 2011, **168**, 22.
- 25 D. Scott and J. Blackwell, *Wear*, 1971, **17**, 323.
- 26 P. J. Blau and R. Komanduri, *J. Eng. Mater. Technol.*, 1990, **112**, 254.
- 27 B. A. Krick, D. W. Hahn and W. G. Sawyer, *Tribol. Lett.*, 2012, **49**, 95.
- 28 M. Gao, Y. Li and J. Choi, *Nano Energy*, 2022, **103**, 107851.



29 L. Zhang, H. Cai, L. Xu, L. Ji, D. Wang, Y. Zheng, Y. Feng, X. Sui, Y. Guo and W. Guo, *Matter*, 2022, **5**, 1532.

30 Y. Bai, X. Guo, B. Tian, Y. Liang, D. Peng and Z. Wang, *Adv. Sci.*, 2022, **9**, 2203249.

31 J.-C. Zhang, X. Wang, G. Marriott and C.-N. Xu, *Prog. Mater. Sci.*, 2019, **103**, 678.

32 A. J. Walton, *Adv. Phys.*, 2006, **26**, 887.

33 Z. Li, Y. Yan, T. Wang, S. Wang, L. Guo, W. Feng, L. Zhao, Z. Wang, F. Zhao, J. Chen, Z. Zhang, X. Xu and X. Yu, *J. Rare Earths*, 2023, **41**, 1869.

34 H. Lv, Y. Wang, Z. Pan, X. Li and Y. Zhang, *J. Rare Earths*, 2023, **41**, 639.

35 X. Pan, Y. Zhuang, W. He, C. Lin, L. Mei, C. Chen, H. Xue, Z. Sun, C. Wang, D. Peng, Y. Zheng, C. Pan, L. Wang and R.-J. Xie, *Nat. Commun.*, 2024, **15**, 39.

36 B. Tian, Z. Wang, A. T. Smith, Y. Bai, J. Li, N. Zhang, Z. Xue and L. Sun, *Nano Energy*, 2021, **83**, 105860.

37 S. Yu, S. Fang, L. Zhao, Y. Bai, R. Wang and Z. Wang, *Chem. Eng. J.*, 2023, **474**, 145542.

38 C.-N. Xu, X.-G. Zheng, M. Akiyama, K. Nonaka and T. Watanabe, *Appl. Phys. Lett.*, 2000, **76**, 179.

39 C.-N. Xu, T. Watanabe, M. Akiyama and X.-G. Zheng, *Appl. Phys. Lett.*, 1999, **74**, 2414.

40 Y. Wang, W. Yang, H. Chen, X. Zhong, G. Zeng, Y. Li and C. Hou, *Chin. J. Lumin.*, 2022, **43**, 1609.

41 H. Xu, F. Wang, Z. Wang, H. Zhou, G. Zhang, J. Zhang, J. Wang and S. Yang, *Tribol. Lett.*, 2019, **67**, 13.

42 J. Li, Z. Zhang, X. Luo, L. Zhu and Z. L. Wang, *ACS Appl. Mater. Interfaces*, 2022, **14**, 4775.

43 W. Ferdous, A. Manalo, T. Aravinthan and G. V. Erp, *Constr. Build. Mater.*, 2016, **124**, 287.

44 Z. Lin, K. Zhang, J. Ye, X. Li, X. Zhao, T. Qu, Q. Liu and B. Gao, *Wear*, 2022, **490–491**, 204178.

45 S. J. Shiao, W. S. Fu, C. L. Tuo and U. I. Cheng, *J. Appl. Polym. Sci.*, 2001, **80**, 1514.

46 J. Khedkar, I. Negulescu and E. I. Meletis, *Wear*, 2002, **252**, 361.

47 X. Zhou, Y. Gao, Y. Wang, P. Xiao and X. Huang, *Wear*, 2022, **506–507**, 204465.

48 W. Qiu, W. Zhao, L. Zhang, H. Wang, N. Li, K. Chen, H. Zhang and Y. Wang, *Adv. Funct. Mater.*, 2022, **32**, 2208189.

